Supplementary Materials for

An isoform of Dicer protects mammalian stem cells against multiple RNA viruses

Enzo Z. Poirier*, Michael D. Buck, Probir Chakravarty, Joana Carvalho, Bruno Frederico, Ana Cardoso, Lyn Healy, Rachel Ulferts, Rupert Beale, Caetano Reis e Sousa*

*Corresponding author. Email: enzo.poirier@crick.ac.uk (E.Z.P.); caetano@crick.ac.uk (C.R.S.)

Published 9 July 2021, *Science* **373**, 231 (2021)
DOI: 10.1126/science.abg2264

This PDF file includes:

Materials and Methods

Cell lines and mouse strains

BHK-21 cells, 3T3 cells, HeLa cells, U2OS cells, Vero cells and HEK293T cells were obtained from the Francis Crick Institute Cell Services Science Technology Platform. KUXP1 human induced pluripotent stem cells (iPSCs) and H9 embryonic stem cells were obtained from the Francis Crick Institute Human Embryo and Stem Cell Unit. Dicer$^{+/+}$aviD$^{+/+}$ and Dicer$^{-/-}$ aviD$^{-/-}$ mouse embryonic stem cells were a gift from Dr. Sara Macias (University of Edinburgh). "NoDice" HEK293T Dicer$^{-/-}$aviD$^{-/-}$were provided by Dr. Bryan Cullen (Duke University). All cells were negative for mycoplasma. BHK-21 cells, Vero cells, 3T3 cells and HEK293T cells were cultured in Dulbecco's modified Eagle's medium (DMEM, Life Technologies) supplemented with 10% fetal calf serum (FCS, Autogen Bioclear UK), 100 U/ml penicillin, 100 U/ml streptomycin (P/S), 2 mM glutamine and incubated at 37ºC with 10% CO_2. Mouse embryonic stem cells were cultured on gelatin-coated plates, in Glasgow minimum essential medium (GMEM, Sigma) supplemented with 10% stem-cell qualified FCS (Life Technologies), 0.1 mM β-mercaptoethanol (Gibco, Life Technologies), 100 U/ml P/S, 1 mM sodium pyruvate (Gibco, Life Technologies), non-essential amino acids (Gibco, Life Technologies), 2 mM glutamine and 1000 U/ml of ESGRO leukemia inhibitory factor (Millipore), at 37ºC with 10% CO_2. Human iPSCs were cultured in vitronectin-coated plates, in Essential 8 medium (Thermo Fisher Scientific) supplemented with 100 U/ml P/S. Neural stem cells were isolated from C57BL6/J mice by digesting the central nervous system into a single-cell suspension using Neural Dissociation kit (P) (Miltenyi Biotech). Cells were cultured in DMEM/F-12 (Thermo Fisher Scientific) supplemented with 0.015 M KCl, 1% BSA, Neurocult (Stem Cell Technologies), 10 ng/ml bFGF (Peprotech), 20 ng/ml EGF (Peprotech), 2 μg /ml heparin (Sigma Aldrich), 100 U/ml P/S and 2 mM glutamine. After 14 days, neurospheres were dissociated with StemPro Accutase (Thermo Fisher Scientific) and plated in flasks pre-coated with DMEM/F-12 supplemented with N-2 Max supplement (R&D Systems), 10 ng/ml bFGF, 20 ng/ml EGF, 5 μg /ml heparin, 2 μg /ml laminin (Sigma Alrich), 100 U/ml P/S and 2 mM glutamine. Neural stem cells were differentiated into astrocytes by adding 20 ng/ml murine BMP-4 (Peprotech) for 4 days.

Organs harvested from adult mice were from 6-12-week old C57BL6/J mice or Lgr5-eGFP-IRES-creERT2 mice. Organs harvested from pups were from one-week old C57BL6/J pre-weaning mice. All mice were bred at the animal facility of the Francis Crick Institute in accordance

with national and institutional guidelines for animal care approved by the Francis Crick Institute Biological Resources Facility Strategic Oversight Committee (incorporating the Animal Welfare and Ethical Review Body) and by the Home Office, UK.

Constructs and complementation

aviD was cloned into a pcDNA3.1(+) vector from purified mouse neural stem cell RNA. Dicer(CD) and aviD(CD) were generated by mutating the GDD catalytic motif (D1310A and D1693A) using QuickChange XL Site-Directed Mutagenesis kit (Agilent), according to the manufacturer's instruction.

To complement Dicer$^{-/-}$aviD$^{-/-}$ HEK293T cells or ES cells, sequences encoding Dicer or aviD were subcloned into a pSBbi-GH plasmid (Addgene #60514) additionally encoding for GFP and hygromycin resistance. 5 x 10^5 Dicer$^{-/-}$aviD$^{-/-}$ NoDice cells or mouse ES cells were transfected with 1.9 µg of pSBbi-GH-Dicer/aviD and 100 ng of pSB100 plasmid encoding for the sleeping beauty transposase, expanded and single-cell sorted for high GFP expression in 96-well plate using a MoFlo XDP Cell Sorter (Beckman Coulter). In the case of ES cells, they were selected for two weeks in 800 µg/ml hygromycin before single-cell sorting. Individual clones were validated for expression of the constructs. Sub-clones of these were further engineered to express ACE2 by transfecting pSBbi-bla (Addgene #60526) expressing human ACE2, selected with 10 µg/ml blasticidin for 48 h, and sorted for equivalent ACE2 and GFP expression.

To generate lines expressing doxycycline-inducible Dicer, aviD or aviD(CD), we made use of Lenti-X Tet-On Advanced Lentiviral System (Clontech). VSV-G-pseudotyped lentivirus was generated by transfecting 70-80% confluent 293T cells with 20 µg of Lenti-X Tet-On plasmid bearing Dicer, aviD or aviD(CD), 6 µg of pMD2.G (Addgene #12259) and 14 µg of psPAX2 (Addgene #12260). Supernatant was collected 48-72 h post transfection, spun down to remove debris and used to transduce Dicer$^{-/-}$aviD$^{-/-}$ HEK293T cells. After 24 h, cells were selected with neomycin and puromycin and single-cell cloned.

Viruses and viral infection

Sindbis virus was produced from the pTR339 infectious clone (*31*), and Zika virus from the pMR766 infectious clone (*32*). SINV-GFP was obtained from the pTE3'2J clone (*33*). WR strain of vaccinia virus was a gift of the Way lab (Francis Crick Institute) and herpes simplex virus

1 is from ATCC (VR-1493). SINV-B2 was generated by replacing GFP in the SINV-GFP sequence by HA-tagged B2 protein using the XbaI cloning sites. *In vitro* transcribed RNA was produced using mMessage mMachine kit (Ambion) with linearized DNA as a template. Purified RNA was transfected into BHK-21 (for SINV) or Vero cells (for ZIKV). Supernatant was then used to infect fresh cells to produce a viral stock that was titrated by plaque assay. Briefly, 24-well plates seeded with 200,000 Vero cells were infected with 10-fold dilutions of sample, overlaid with DMEM supplemented with 2% FCS, 100 U/ml P/S and 0.8% agarose, and incubated for 2 days (SINV) or 5 days (ZIKV). Cells were fixed with 10% formalin and stained with crystal violet. SARS-CoV-2 was amplified from a positive patient sample on Vero E6 cells. Titre was determined by measuring the number of N gene copies by RT-qPCR with respect to a standard obtained from the National Institute for Biological Standards and Control (UK).

Cells were infected by overlaying the adequate amount of virus (MOI indicated in figure legends or in Materials and Methods) diluted in DMEM without FCS and incubating 1 h at 37ºC. Cells were then washed 3 times with PBS before culture in regular medium containing FCS. For infection of doxycycline-inducible cells, cells were incubated with 1 µg/ml doxycycline overnight prior to infection with SINV-GFP at MOI 3. Organoids were infected with 3×10^5 PFU of ZIKV or 10^7 N gene copies of SARS-CoV-2 in differentiation media containing vitamin A.

RNA extraction and RT-PCR and qPCR

RNA extraction from mouse tissues was performed using RNeasy Mini Kit columns (Qiagen) following the manufacturer's instructions, including a DNase treatment step. Cell line RNA was extracted using TRIzol reagent (Invitrogen) according to the manufacturer's instructions. Reverse transcription of 200 ng RNA was performed with the SuperScript Reverse Transcriptase kit (Thermo Fisher Scientific) using random hexamers or primers specific for a given miRNA: miR-21 (RT000397), let-7a (RT000377), miR-155 (RT002571), miR-146a (RT000468). miR-673 measurement was performed by using the Taqman Advanced miRNA cDNA Synthesis kit (Thermo Fisher Scientific) according to the manufacturer's instructions. Dicer/aviD amplicons were amplified by PCR using Phusion Hot Start II DNA Polymerase (Thermo Fisher Scientific) with primers 5'-TTAACCTTTTGGTGTTTGATGAG-3' and 5'-CTCCTCGTCATGTAAGTCCAGC-3'. cDNA was diluted 1:2 in water and probed by qPCR using TaqMan Gene Expression Assays (Thermo Fisher Scientific) on a QuantStudio 7 Flex

(Applied Biosystems). The following probes were used: mouse Dicer (Mm00521715_m1), mouse aviD (APT2AK7) (Primers 5'-AGGAGTGACGCTGAGAC-3' and 5'-CAGCTCTGGATCTTGTTTG-3', VIC probe TGGTCCTGGACAGATTGATAAAGGAA), human Dicer (Hs00998590_m1), human aviD (APH6A96) (Primers 5'-GAGTAATGCTGAAACTGCAA-3' and 5'-AAGCCAGCTCTGGATCTT-3', VIC probe TGGTGGTCTTAGACAGATTGATAAAGGAA), mouse MDA5 (Mm00459183_m1), mouse IFIT1 (Mm00515153_m1), mouse Viperin (Mm00491265_m1), mouse GAPDH (Mm99999915_g1), human actin (Mm999999032_m1), human GAPDH (Hs03929097_g1), SARS-CoV-2 N gene (Primers 5'-TCTGGTAAAGGCCAACAACAA-3' and 5'-TGTATGCTTTAGTGGCAGTACG-3', FAM probe CTGTCACTAAGAAATCTGCTGCTGAGGC), miR-21 (TM000397), let-7a (TM000377), miR-155 (TM002571), miR-146a (TM000468), miR-673 (TM002054).

Western blot

Cells were washed in cold PBS and pelleted for 5 min at 1,400 x *g*. Pellet was resuspended in lysis buffer (20 mM Tris-HCl pH 8, 150 mM NaCl, 5 mM EDTA freshly supplemented with 1% NP-40 and Halt-Protease Inhibitor Cocktail from Thermo Fisher Scientific, 78425) at 100 x 10^6 cells/mL and incubated on ice for 30 min. Debris were remove by centrifugation at 18,000 x *g* for 15 min at 4°C. Supernatant was mixed 1:1 with 2X Laemmli Sample Buffer (Bio-Rad, 161-0737) supplemented with β-mercaptoethanol and boiled for 5 min, before being resolved on 4-20% or 7.5% TGX precast gels (Bio-Rad). To resolve Dicer from aviD, samples were run on 7.5% TGX precast gels for 5 h at 70 V, or until the 75 kDa band of the Precision Plus Protein Dual Color Standard (Bio-Rad, 1610374) reached the bottom of the gel. Proteins were transferred to a PVDF membrane with a Trans-Blot Turbo Transfer System (Bio-Rad, 1704150). The membrane was blocked in 5% bovine serum albumin in TBS, 0.1% tween-20 and incubated at 4°C overnight with primary antibodies against the following proteins: Dicer [N167/7] (Abcam, ab 167444) at 1:1000, Ago2 (Cell Signaling Technology, C4C36 at 1:1000). Secondary antibodies anti-mouse-HRP (Invitrogen 21040) or anti-rabbit-HRP (Southern Biotech 4050-05) at 1:10,000, as well as anti-FLAG-HRP (clone M2, Sigma) or anti-β-actin-HRP (13E5, Cell Signaling Technology) were added for one hour at room temperature. Detection was performed with Luminata Forte Western HRP Substrate (Millipore) using an Amersham Imager 600.

Purification of recombinant Dicers and *in vitro* dicing assay

Recombinant Dicer, Dicer(CD) and aviD were purified as described in Maillard *et al.* (*19*). Briefly, HEK293T were transfected with pcDNA3.1(+) encoding FLAG-tagged proteins. Proteins were immunoprecipitated using anti-FLAG M2 antibody, washed extensively before elution, concentration and measurement of protein content using a Pierce BCA Protein Assay kit. Cy5-tagged long dsRNA was prepared from the first 200 nucleotides of GFP, as described in van der Veen *et al.* (*20*). *In vitro* dicing assay was performed by incubating 50 nM of dsRNA with 500 nM recombinant protein in 30 mM Tris pH 6.8, 50 mM NaCl, 3 mM $MgCl_2$, 5% glycerol, 4 mM DTT, RNaseIn (Promega) for the indicated time point at 37ºC. RNA was extracted by phenol/chlorophorm purification, resuspended in 47.5% formamide, 0.01% SDS, 0.01% bromophenol blue, 0.5 mM EDTA and resolved on a 10% TBE-Urea gel (Thermo Fisher Scientific) and visualized by in-gel fluorescence with an Amersham Imager 600.

siRNA and poly(I:C) transfection

25,000 cells were plated in 24-well plates and transfected with 1.25 µl of siGENOME control siRNA (D-001210-01-05, Dharmacon) or siGENOME siRNA human EIF2C2 targeting Ago2 (D-001210-01-05) at 20 µM, using DharmaFECT 1 (Horizon), according to the manufacturer's instructions. Medium was replaced after 4 h, and transfected cells were infected 24 h later. 400,000 ES cells were transfected with 1 µg poly(I:C) using Lipofectamine 2000 (Thermo Fisher Scientific) according to the manufacturer's instructions. Cells were collected 5 h post transfection, RNA was extracted using TRIzol and used for RT-qPCR studies.

Flow cytometry

Cells were collected by trypsin-EDTA treatment into a V-shape bottom 96-well plate (Corning), fixed and permeabilized using Fix & Perm kit 1000 (Nordic MUbio). Briefly, cells were resuspended in 50 µl PBS supplemented with DAPI, then mixed with 100 µl of Fixation Buffer A, for 15 min at room temperature. Cells were washed once in PBS, then resuspended in Permeabilization buffer B supplemented with anti-FLAG-PE diluted 1:300 (BioLegend, 637310), washed 3 times with PBS and resuspended in 100 µl of FACS buffer (PBS, 2% FCS, 2 mM EDTA). Analyses were performed on an LSR Fortessa (BD Biosciences), with at least 10,000 cells acquired. Data analysis was performed with FlowJo (TreeStar). ACE2 staining was performed

prior to fixation by incubating cells in FACS buffer supplemented with 1 µl/ml of biotinylated SARS-CoV-2 Spike protein (Acro Biosystems) and streptavidin conjugated to Alexa-647 (Invitrogen) at 1:400, for 30 min at 4°C.

In situ hybridization by BaseScope

In situ hybridization was performed using the BaseScope platform (ACD) following the manufacturer's instructions, on samples fixed in formaldehyde for 16 h, paraffin-embedded and cut into 5 µm thick slices. aviD mRNA was detected using a customized probe (catalogue number 718198) and GFP was detected by immunofluorescence using an anti-GFP antibody (Abcam, ab6673). 4-hydroxy-terahydrodipicolinate reductase (dapB) probe, which targets a bacterial enzyme mRNA, was used as a negative control. Peptidyl-prolyl cis-trans isomerase B (PPIB) probe was used as a positive control. Images were acquired on a LSM880 inverted confocal microscope (Zeiss).

Quantification of mRNA by PrimeFlow cytometry

Brain organoid single cell suspension was generated via papain dissociation (*34*) using the Worthington Papain Dissociation System kit (Worthington Biochemicals) according to the manufacturer's instructions. Small intestine single cell suspension was generated by adapting protocols from Gracz *et al.* (*35*, *36*). Mouse small intestine was isolated in ice-cold PBS, open longitudinally and washed with PBS before removing villi by scraping. Tissues were incubated on ice in PBS, 30 mM EDTA, 1.5 mM DTT, 10 µM Y27632 (Sigma Aldrich) for 20 min, then in PBS, 30 mM EDTA, 10 µM Y27632 for 10 min at 37°C. Tubes were shaken for 30 s to release epithelial cells from basement membrane and pelleted at 1000 x *g* for 5 min at 4°C. Cells were washed in DMEM/F-12 with HEPES, P/S and Glutamax (ADMEM+++) and passed through a 70 µm filter, before being incubated in 10 mg Collagenase/Dispase (Sigma Aldrich) for 10 min at 37°C, shaking for 30 s every 2 min. The resulting suspension was supplemented with 10% FBS and 0.5 mg of DNase I (Roche) and sequentially passed through a 70 µm and 40 µm filters. Cells were washed once with ADMEM+++ media and once with FACS buffer, then processed for PrimeFlow cytometry. Skin single cell suspensions were generated from mouse ears as described by Cardoso *et al.* (*37*), digesting for 30 min with 0.25 mg/ml Liberase TL (Roche) and 0.1 mg/ml DNase I (Roche). Digested dermis was scraped onto a 70 µm filter soaked in cold PBS. The

resulting suspension was passed through a 40 µm filter twice and washed twice with FACS buffer before PrimeFlow processing. Hippocampi were dissected under a stereoscope and collected into ice-cold HBSS-media (Invitrogen). Single-cell suspension was generated using Neural Tissue Dissociation kit (P) (Miltenyi Biotec) following the manufacturer's instructions.

Staining of mRNA was performed using PrimeFlow RNA assay kit (Thermo Fisher Scientific) in V bottom-shaped 96-well plates according to the manufacturer's instruction, including a pre-treatment with PrimeFlow microRNA Pretreatment Buffer (Thermo Fisher Scientific). The following mRNAs were detected: Dicer mRNA with a type 10 probe targeting exons 7 and 8 absent in aviD mRNA (VP7DPEH), aviD with a customized type 1 probe (VP7DPEF), Sox2 with a type 4 probe (VB4-18399-PF) and eGFP with a type 4 probe (VF4-13750).

Brain organoids

A protocol from Lancaster *et al.* (*38*) was adapted to generate brain organoids from mouse ES cells. Briefly, Dicer$^{+/+}$aviD$^{-/-}$ and Dicer$^{-/-}$aviD$^{+/+}$ ES cells were incubated in 0.8 mg/ml hygromycin for 48 h. 9,000 cells were plated in 96-well U-bottom ultralow attachment plate (Corning, CLS3473) with 5 vicryl fibers (Johnson&Johnson, W9067) around 0.5 cm in length, in 150 µl of GMEM, 10% knock-out serum, 2 mM glutamine, 1 mM pyruvate, 0.1 mM non-essential aminoacids, 0.1 mM ß-mercaptoethanol, 10 µM SB431542 (Sigma Aldrich). Medium was replenished after 48 h. Four days post plating, embryonic bodies were transferred to 24-well ultralow attachment plates (Corning) containing 500 µl of neural induction media (DMEM/F-12 with 1% N2 supplement, 1% GlutaMAX supplement [Invitrogen, 35050-038], 1% MEM-NEAA and 1 µg/ml heparin [Sigma, H3149]). Embryonic bodies were transferred in Matrigel (BD Biosciences) after 48 h, in a 6-cm dish (Corning) containing 5 ml of differentiation media without vitamin A (50% DMEM/F-12, 50% Neurobasal media [Invitrogen], 0.5% N2 supplement, 0.025% insulin [Sigma, 19278], 0.5% MEM-NEAA, 1% P/S, 17.5 µM ß-mercaptoethanol, 1% B27 – vitamin A supplement [Invitrogen, 12587010]). Medium was changed after 48 h. After an additional 48 h, growth medium was changed to differentiation medium with vitamin A (B27 + vitamin A supplement, Invitrogen, 17504044) and dishes were transferred to an orbital shaker at 85 r.p.m.

Immunofluorescence

Immunofluorescence on uninfected cells or SARS-CoV-2-infected cells was performed by plating 50,000 cells on 13 mm poly-L lysine-coated coverslips (VWR, 631-0150). After 24 h, cells were infected with an inoculum containing 10^7 N gene copies of SARS-CoV-2, for 1 h in serum free DMEM. Cells were fixed with 4% PFA in PBS for 30 min, washed 3 times with PBS and incubated with 0.3% Triton X-100 (Sigma Aldrich) in PBS for 1 h at room temperature. After 3 washes, cells were blocked with 3% BSA in PBS for 1 h. Cells were then incubated with antibody diluted in blocking buffer for 1 h at room temperature, washed three times with PBS for 5 min and incubated with secondary antibodies at 1:400 and Hoechst dye diluted blocking buffer. After 3 PBS washes, coverslips were mounted on Microscope slides (Scientific Glass Laboratories Ltd) with ProLong Diamond Antifade Mountant (Invitrogen). For organoids, samples were fixed in PBS with 4% PFA for 30 min, washed 3 times for 10 min each with PBS and incubated overnight in 30% sucrose in PBS. Organoids were then embedded in Optimal Cutting Temperature compound (VWR Chemicals) and cut into 40 µm thick slices using a cryostat (Leica, CM3050S), then transferred on PolyFrost Microslides (Solmedia). After incubation in PBS for 10 min at room temperature, samples were incubated with blocking buffer (3% BSA, 0.3% Triton X-100 in PBS) for 1 h. Primary antibodies were diluted in blocking buffer and overlayed on samples for 1 h at room temperature, before being washed out (3 times, 5 min in PBS). Samples were then incubated with secondary antibodies diluted 1:400 and Hoechst dye at 1:2000 in blocking buffer for 1 h at room temperature. Mounting was performed with ProLong Diamond Antifade Mountant and 0.16-0.19 mm thick glass coverslips (Academy). Primary antibodies used were anti-Sox2 (AF2018, R&D Systems) at 1:500, anti-Sox2-Alexa488 (53-9811-82, Invitrogen) at 1:200, anti-dsRNA (9D5, Absolute Antibody) at 1:500, anti-Flavivirus Group Antigen (MAB10216, Millipore) at 1:500, anti-SARS-CoV-2 N protein (CR3009, in-house production) at 1:500, anti-TUBB3 (802001, Biolegend) at 1:100, anti-FLAG-Cy3 (A9594, Sigma Aldrich) at 1:500 and anti-GFAP (GA52461-2, Agilent) at 1:500. Secondary antibodies were donkey anti-goat-Alexa488 (A32814, Invitrogen), donkey anti-rabbit-Alexa647 (A32795, Invitrogen), anti-mouse Fab2-Alexa555 (Cell Signaling Technology, 4409S). EdU was visualized using the Click-iT Plus EdU Alexa Fluor 594 Imaging kit (C10639, Thermo Fisher Scientific). Images were acquired on a LSM880 inverted confocal microscope.

Small RNA sequencing

Individual Dicer$^{+/+}$aviD$^{+/+}$, Dicer$^{+/+}$aviD$^{-/-}$ and Dicer$^{-/-}$aviD$^{+/+}$ brain organoids were infected with ZIKV or SARS-CoV-2 and collected after 4 days. RNA extraction was performed from organoids ground in 2 ml Eppendorf tubes containing 500 µl TRIzol reagent and one Stainless Steel 5 mm bead (Qiagen) using a TissueLyser LT (Qiagen) at 50 oscillations/s for 1 min. For ZIKV-infected organoids, 400 ng of RNA was processed for next-generation sequencing using the HiSeq 4000 platform (Illumina). 10^8 reads were sequenced per sample, generating ~26 million 100 bp single-end reads per sample. For SARS-CoV-2-infected organoids, next-generation sequencing was performed by Fasteris (1255 Veyrier, Switzerland). Small RNAs were enriched by polyacrylamide gel selection and RNA was processed for next-generation sequencing using the NextSeq 500 platform (Illumina). 10^8 reads were sequenced per sample generating ~30 million 75 bp single-end reads per sample. Reads were trimmed to 40 bp using Cutadapt (version 0.1.9) (*39*). In addition to trimming the read length, quality trimming (-q 20), adaptor removal (-a 'AGATCGGAAGAGC') and reads shorter than 18 bp were excluded (-m 18). Reads were mapped to the ZIKV genome (GenBank: MK105975.1) using Bowtie (version 1.2.0) (*40*) with default parameters with one mismatch (-v 1). BAM files were created using Samtools version 1.3.1 (*41*). Coverage over ZIKV genome was determined using mapped 22 bp reads only, using BEDTools's genome CoverageBed function. version 2.27.1 (*42*). Reads mapping to the first 500 bp of the ZIKV genome were extracted and further analyzed for overlapping reads on the positive and negative strand. Radial plots were drawn using R version 3.6.0 (https://www.r-project.org) and the 'plotrix' library (*43*), showing the frequency of overhangs of overlapping reads.

Image and statistical analysis

Image analysis was performed on Fiji (version 2.0.0-rc-69/1.52p, https://imagej.net/Fiji).

All statistical tests were performed on GraphPad Prism version 7 (https://www.graphpad.com). *P* values < 0.05 were considered significant.

Figure S1

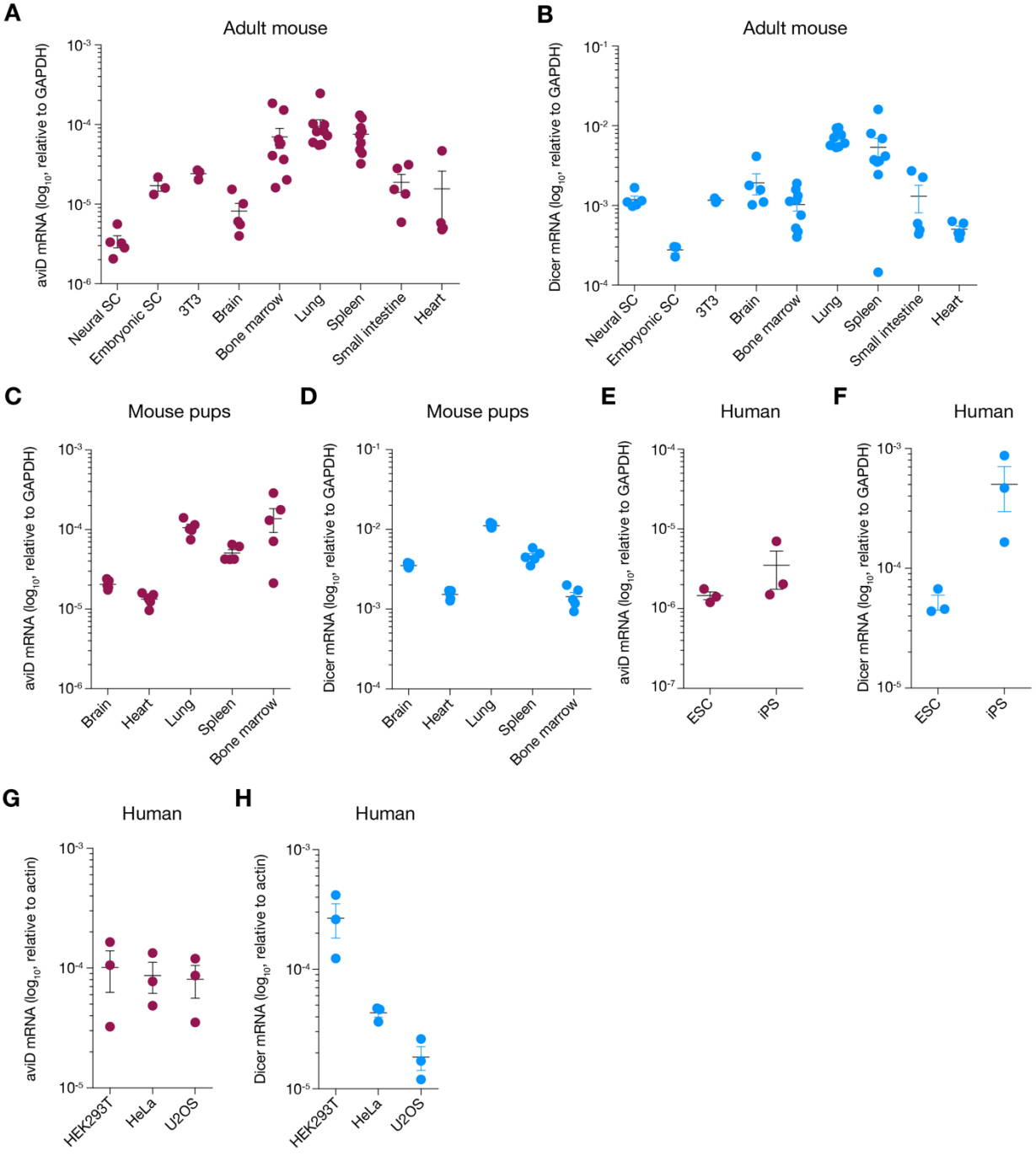
A
Adult mouse
aviD mRNA (log10, relative to GAPDH)
Neural SC
Embryonic SC
3T3
Brain
Bone marrow
Lung
Spleen
Small intestine
Heart
B
Adult mouse
Dicer mRNA (log10, relative to GAPDH)
C
Mouse pups
D
Mouse pups
E
Human
aviD mRNA (log10, relative to GAPDH)
ESC
iPS
F
Human
Dicer mRNA (log10, relative to GAPDH)
G
Human
aviD mRNA (log10, relative to actin)
HEK293T
HeLa
U2OS
H
Human
Dicer mRNA (log10, relative to actin)

Fig. S1. aviD mRNA is expressed in mice and humans.

(**A**) aviD or (**B**) Dicer mRNA was measured by RT-qPCR in the indicated mouse cell line or tissues from 6-10 weeks old C57BL6/J mice. (**C**) aviD or (**D**) Dicer mRNA was measured by RT-qPCR in the indicated organs from 1 week-old mouse pups. (**E,G**) aviD or (**F,H**) Dicer mRNA was measured by RT-qPCR in the indicated human cell line. Data points are biological replicates. Horizontal bars are mean ± SEM.

Figure S2

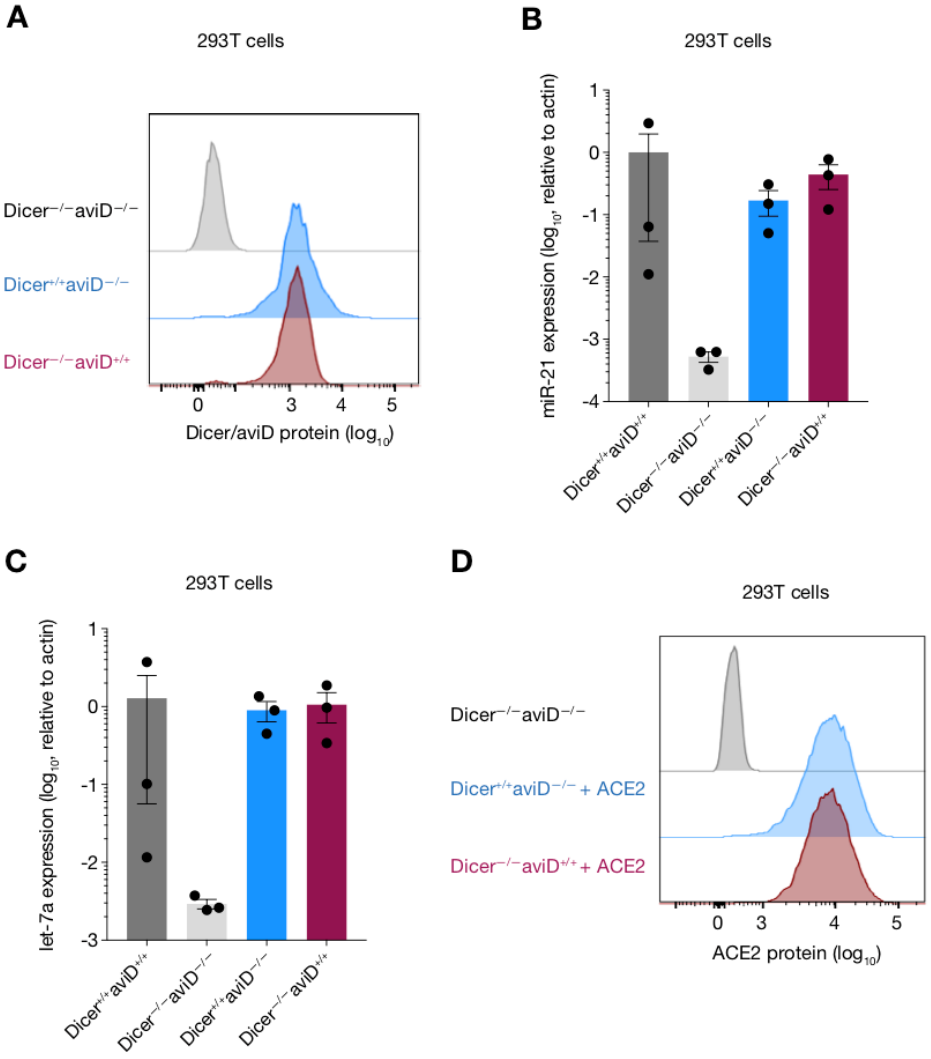
A
293T cells
Dicer−/−aviD−/−
Dicer+/+aviD−/−
Dicer−/−aviD+/+
0
3
4
5
Dicer/aviD protein (log10)
B
293T cells
miR-21 expression (log10, relative to actin)
1
0
-1
-2
-3
-4
Dicer+/+aviD+/+
Dicer−/−aviD−/−
Dicer+/+aviD−/−
Dicer−/−aviD+/+
C
293T cells
let-7a expression (log10, relative to actin)
1
0
-1
-2
-3
Dicer+/+aviD+/+
Dicer−/−aviD−/−
Dicer+/+aviD−/−
Dicer−/−aviD+/+
D
293T cells
Dicer−/−aviD−/−
Dicer+/+aviD−/− + ACE2
Dicer−/−aviD+/+ + ACE2
0
3
4
5
ACE2 protein (log10)

Fig. S2. Expression of Dicer or aviD in Dicer$^{-/-}$aviD$^{-/-}$ HEK293T cells restores miRNA production.

(**A**) HEK293T Dicer$^{-/-}$aviD$^{-/-}$ cells expressing FLAG-tagged Dicer or aviD were generated by transposon-driven genome insertion. Dicer/aviD protein expression was determined via FLAG staining by flow cytometry. Parental Dicer$^{-/-}$aviD$^{-/-}$ cells were used as a negative control. Expression of (**B**) miR-21 or (**C**) let-7a was measured by RT-qPCR in Dicer$^{+/+}$aviD$^{+/+}$, Dicer$^{-/-}$aviD$^{-/-}$, Dicer$^{+/+}$aviD$^{-/-}$ or Dicer$^{-/-}$aviD$^{+/+}$ cells. Data points represent mean and error bars are SEM. (**D**) Dicer$^{+/+}$aviD$^{-/-}$ and Dicer$^{-/-}$aviD$^{+/+}$ HEK293T cells were engineered to stably express the SARS-CoV-2 receptor ACE2. Protein expression was determined by flow cytometry.

Figure S3

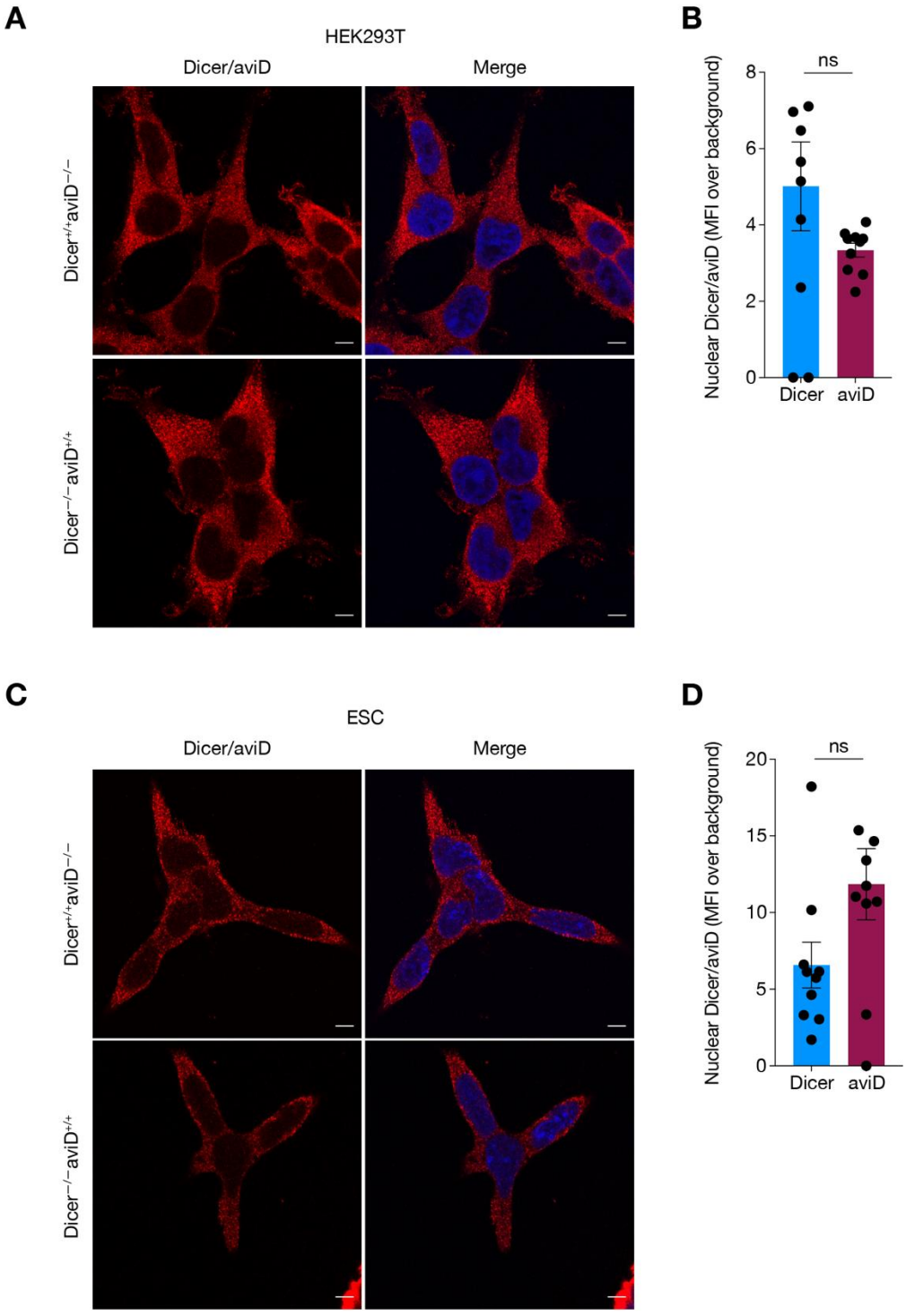
A
HEK293T
Dicer/aviD
Merge
Dicer+/+aviD−/−
Dicer−/−aviD+/+
B
Nuclear Dicer/aviD (MFI over background)
ns
Dicer
aviD
C
ESC
Dicer/aviD
Merge
Dicer+/+aviD−/−
Dicer−/−aviD+/+
D
Nuclear Dicer/aviD (MFI over background)
ns
Dicer
aviD

Fig. S3. Subcellular localisation of Dicer and aviD.

Dicer or aviD localisation was analysed by immunofluorescence in Dicer$^{-/-}$aviD$^{-/-}$ (**A-B**) HEK293T cells or (**C-D**) mouse ES cells complemented with FLAG-tagged Dicer or aviD. Scale bar: 10 µm. (**B,D**) Mean fluorescence intensity (MFI) of Dicer or aviD nuclear signal. Data are normalised against background MFI (from control non-complemented Dicer$^{-/-}$aviD$^{-/-}$ cells). *n* = 10 fields of view with at least 5 cells per field. Data are mean ± SEM. Mann-Whitney test; ns, not significant.

Figure S4

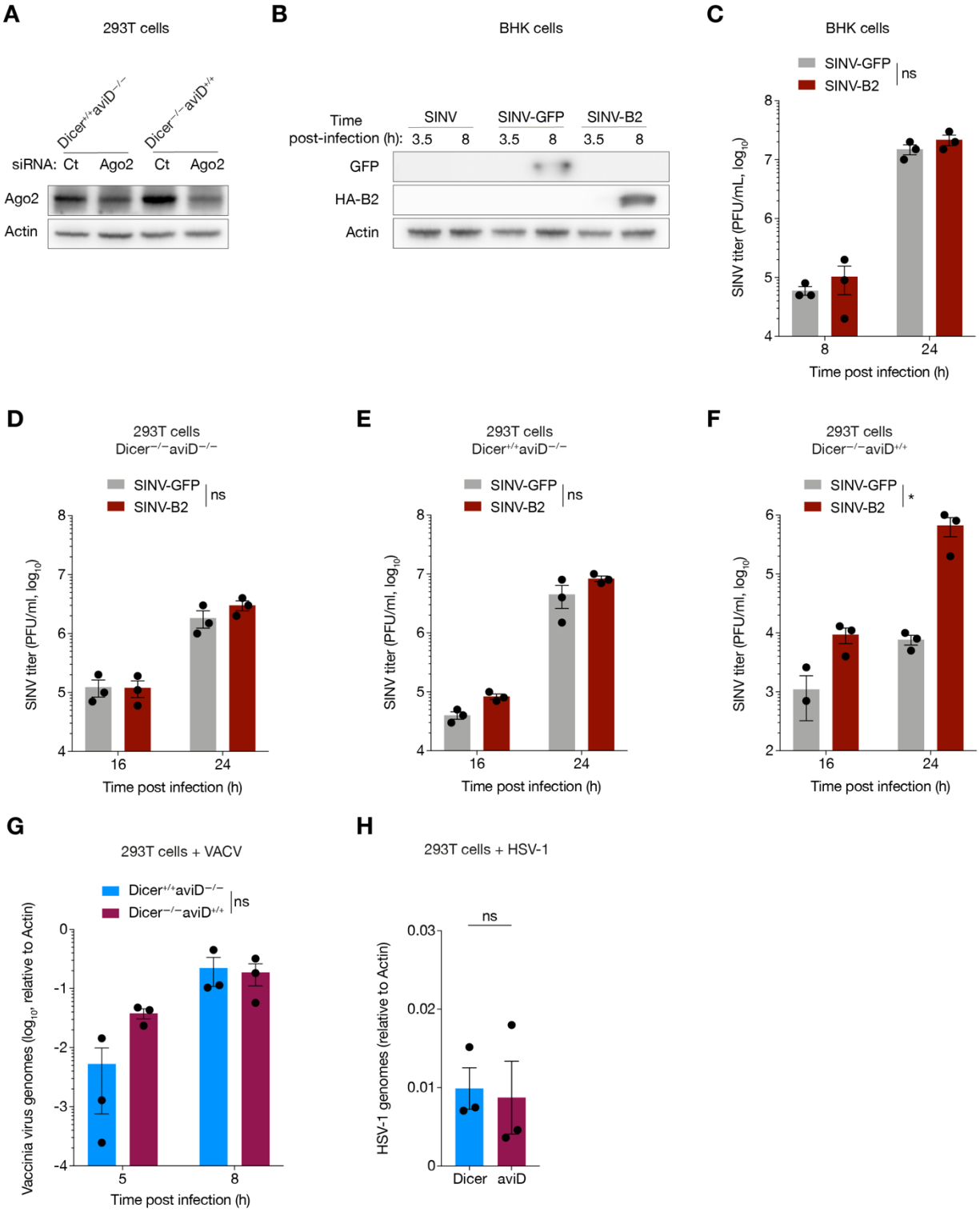
A
293T cells
Dicer+/+aviD−/−
Dicer−/−aviD+/+
siRNA: Ct Ago2 Ct Ago2
Ago2
Actin
B
BHK cells
Time post-infection (h): SINV 3.5 8 SINV-GFP 3.5 8 SINV-B2 3.5 8
GFP
HA-B2
Actin
C
BHK cells
SINV-GFP
SINV-B2
ns
SINV titer (PFU/mL, log10)
Time post infection (h)
D
293T cells Dicer−/−aviD−/−
SINV-GFP
SINV-B2
ns
SINV titer (PFU/ml, log10)
Time post infection (h)
E
293T cells Dicer+/+aviD−/−
SINV-GFP
SINV-B2
ns
SINV titer (PFU/ml, log10)
Time post infection (h)
F
293T cells Dicer−/−aviD+/+
SINV-GFP
SINV-B2
*
SINV titer (PFU/ml, log10)
Time post infection (h)
G
293T cells + VACV
Dicer+/+aviD−/−
Dicer−/−aviD+/+
ns
Vaccinia virus genomes (log10, relative to Actin)
Time post infection (h)
H
293T cells + HSV-1
ns
HSV-1 genomes (relative to Actin)
Dicer
aviD

Fig. S4. Expression of B2 by SINV counteracts aviD-dependent antiviral RNAi.
(**A**) Dicer$^{+/+}$aviD$^{-/-}$ or Dicer$^{-/-}$aviD$^{+/+}$ HEK293T cells were transfected with a siRNA targeting Ago2 or with an unrelated siRNA (Ct). Ago2 expression was assessed by Western blot 24 h post transfection. Actin is shown as a loading control. (**B**) Baby hamster kidney cells (BHK) were infected with parental SINV, SINV expressing HA-tagged B2 protein of Nodamura virus (SINV-B2) or SINV expressing GFP (SINV-GFP) at MOI 0.1, and collected at the indicated time point. GFP and B2 expression were analysed by Western blot using an anti-GFP and an anti-HA antibody, respectively. Actin is shown as a loading control. (**C**) BHK cells, (**D**) Dicer$^{-/-}$aviD$^{-/-}$ cells, (**E**) Dicer$^{+/+}$aviD$^{-/-}$ cells, or (**F**) Dicer$^{-/-}$aviD$^{+/+}$ were infected with SINV-GFP or SINV-B2 at MOI 0.1 (C) or MOI 0.001 (D-F). Supernatant was collected at the indicated time point and was titrated by plaque assay. (**G,H**) Dicer$^{+/+}$aviD$^{-/-}$ cells or Dicer$^{-/-}$aviD$^{+/+}$ were infected with (G) vaccinia virus (VACV) at MOI 4 or (H) herpes simplex virus 1 (HSV-1) at MOI 1 and viral genomes were quantified by qPCR at the indicated time points. Data in A,C-H are from one of three independent experiments. Data are mean ± SEM; $n = 3$ biological replicates. *$P < 0.05$ [two-way ANOVA in (C-G), Mann-Whitney test in (H)].

Figure S5

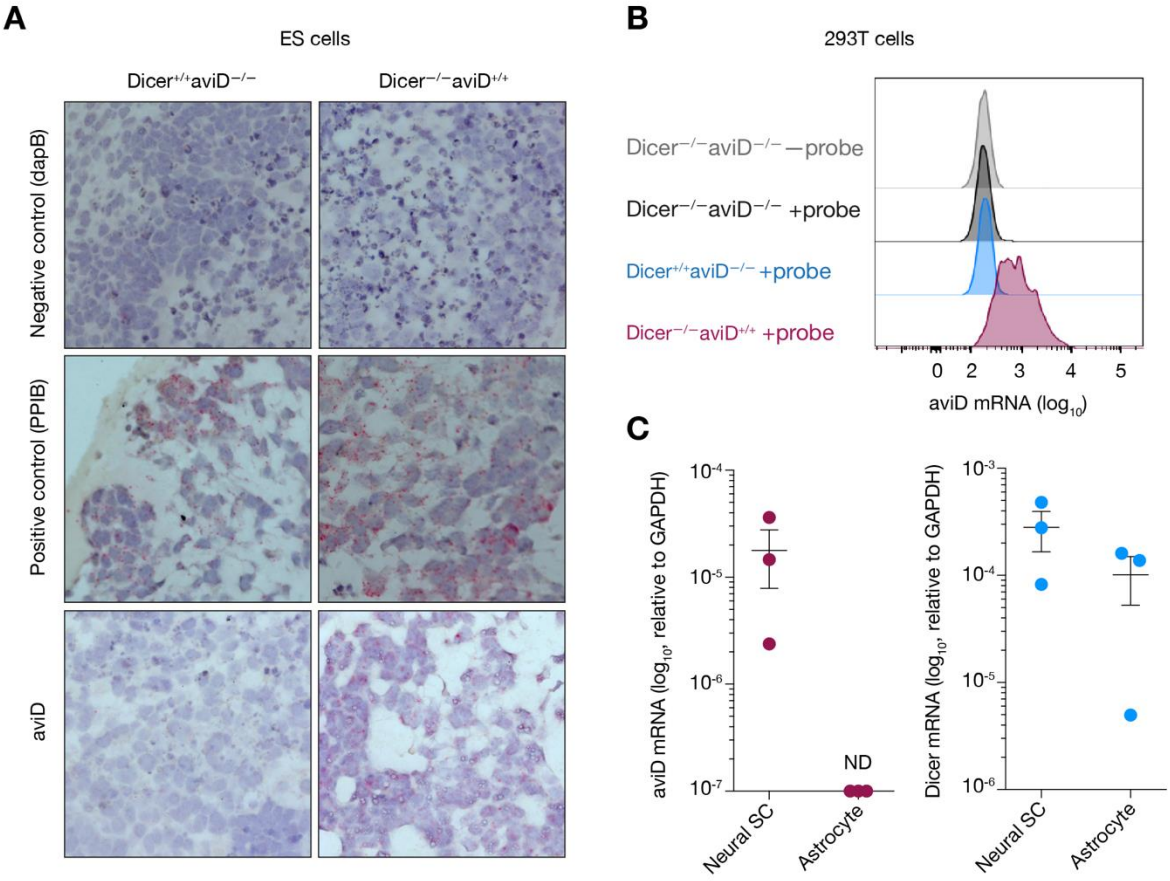
A
ES cells
Dicer+/+aviD−/−
Dicer−/−aviD+/+
Negative control (dapB)
Positive control (PPIB)
aviD
B
293T cells
Dicer−/−aviD−/− —probe
Dicer−/−aviD−/− +probe
Dicer+/+aviD−/− +probe
Dicer−/−aviD+/+ +probe
0 2 3 4 5
aviD mRNA (log10)
C
aviD mRNA (log10, relative to GAPDH)
10-4
10-5
10-6
10-7
ND
Neural SC
Astrocyte
Dicer mRNA (log10, relative to GAPDH)
10-3
10-4
10-5
10-6
Neural SC
Astrocyte

Fig. S5. Detection of aviD mRNA by BaseScope or PrimeFlow cytometry.
(**A**) Mouse ES cells Dicer$^{-/-}$aviD$^{-/-}$ complemented with Dicer (Dicer$^{+/+}$aviD$^{-/-}$) or with aviD (Dicer$^{-/-}$aviD$^{+/+}$) were processed for *in situ* hybridization using the BaseScope platform (ADC Bio). A probe hybridised to a given mRNA appears as a red dot. aviD probe shows specificity as it lights up in Dicer$^{-/-}$aviD$^{+/+}$ but not Dicer$^{+/+}$aviD$^{-/-}$ cells. (**B**) Mouse ES cells Dicer$^{-/-}$aviD$^{-/-}$, Dicer$^{+/+}$aviD$^{-/-}$ or Dicer$^{-/-}$aviD$^{+/+}$ were hybridised with a probe targeting aviD mRNA using the PrimeFlow platform (Thermo Fisher Scientist). aviD probe shows no unspecific background in Dicer$^{-/-}$aviD$^{-/-}$ cells nor does it detect target in Dicer$^{+/+}$aviD$^{-/-}$ cells. (**C**) aviD and Dicer mRNA was quantified by RT-qPCR in neural stem cells and in astrocytes differentiated from neural stem cells in culture. Data are mean ± SEM; n = 3 biological replicates.

Figure S6

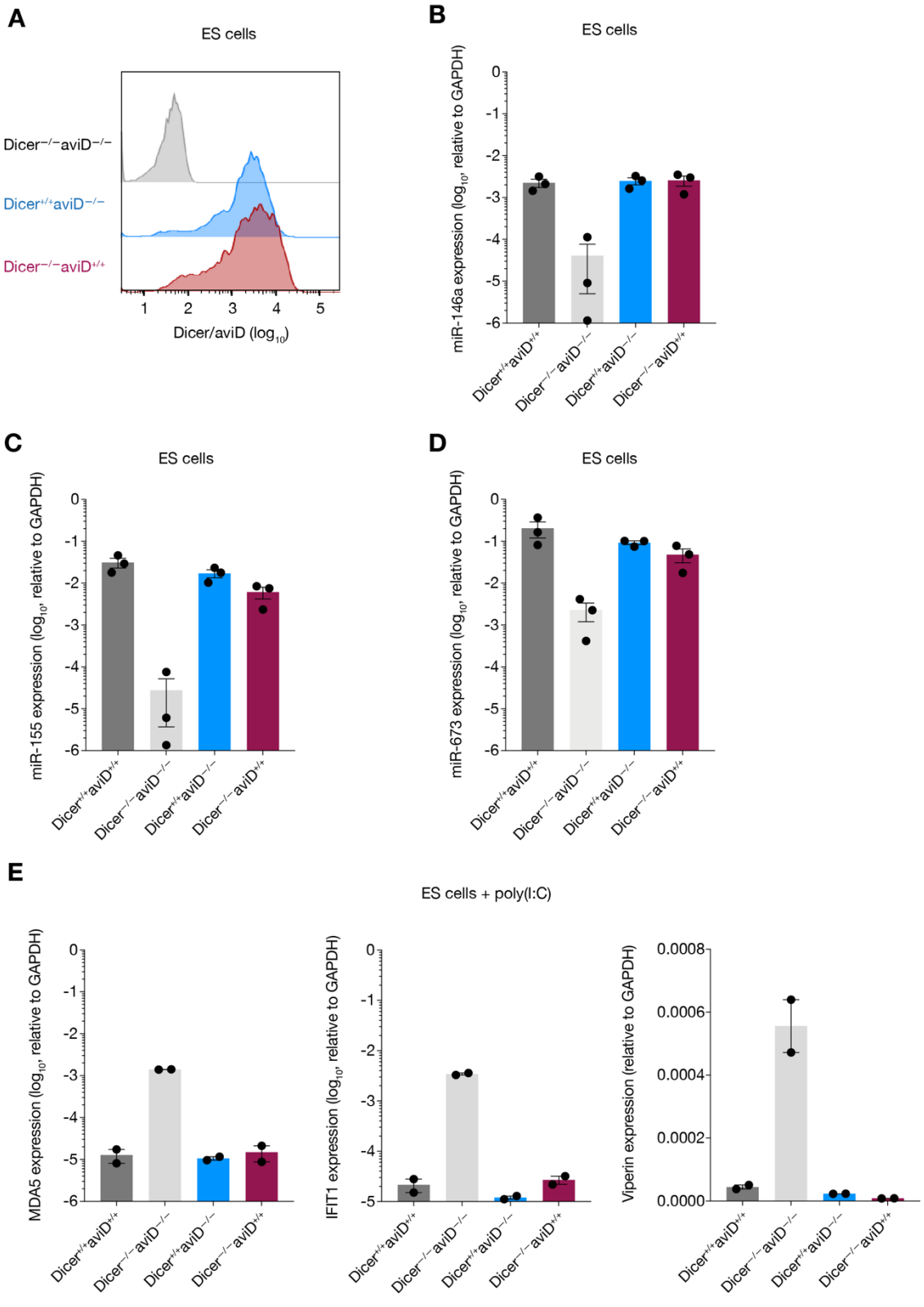
A
ES cells
Dicer−/−aviD−/−
Dicer+/+aviD−/−
Dicer−/−aviD+/+
1
2
3
4
5
Dicer/aviD (log10)
B
ES cells
miR-146a expression (log10, relative to GAPDH)
0
-1
-2
-3
-4
-5
-6
Dicer+/+aviD+/+
Dicer−/−aviD−/−
Dicer+/+aviD−/−
Dicer−/−aviD+/+
C
ES cells
miR-155 expression (log10, relative to GAPDH)
D
ES cells
miR-673 expression (log10, relative to GAPDH)
E
ES cells + poly(I:C)
MDA5 expression (log10, relative to GAPDH)
IFIT1 expression (log10, relative to GAPDH)
Viperin expression (relative to GAPDH)
0.0008
0.0006
0.0004
0.0002
0.0000

Fig. S6. Expression of Dicer or aviD in ES Dicer$^{-/-}$aviD$^{-/-}$ cells restores miRNA production and IFN unresponsiveness.

(**A**) Mouse Dicer$^{-/-}$aviD$^{-/-}$ ES cells were complemented with FLAG-tagged Dicer or aviD by transposon-driven genome insertion. Intracellular FLAG expression determined by flow cytometry. Parental Dicer$^{-/-}$aviD$^{-/-}$ cells are shown as a negative control. Expression of (**B**) miR-146a, (**C**) miR-155 and (**D**) miR-673 was measured by RT-qPCR in Dicer$^{+/+}$aviD$^{+/+}$, Dicer$^{-/-}$aviD$^{-/-}$, Dicer$^{+/+}$aviD$^{-/-}$ or Dicer$^{-/-}$aviD$^{+/+}$ cells. (**E**) The indicated cell types were transfected with poly(I:C) as a mimic of viral infection and collected after 5 hours. Levels of mRNA encoding MDA5, IFIT1 and Viperin were measured by RT-qPCR. Data are mean ± SEM.

Figure S7

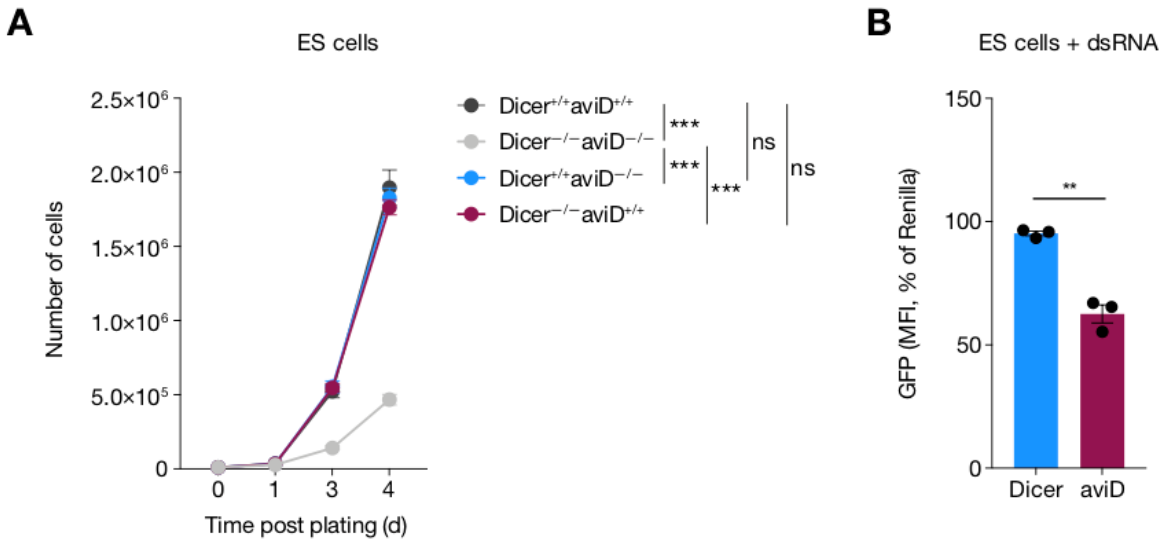
A
ES cells
Number of cells
2.5×10⁶
2.0×10⁶
1.5×10⁶
1.0×10⁶
5.0×10⁵
0
0
1
3
4
Time post plating (d)
Dicer+/+aviD+/+
Dicer−/−aviD−/−
Dicer+/+aviD−/−
Dicer−/−aviD+/+
***
***
***
ns
ns
B
ES cells + dsRNA
GFP (MFI, % of Renilla)
150
100
50
0
**
Dicer
aviD

Fig. S7. Expression of Dicer or aviD in Dicer$^{-/-}$aviD$^{-/-}$ ES cells restores growth.
(**A**) Growth of Dicer$^{+/+}$aviD$^{+/+}$, Dicer$^{-/-}$aviD$^{-/-}$, Dicer$^{+/+}$aviD$^{-/-}$ or Dicer$^{-/-}$aviD$^{+/+}$ ES cells was monitored over 4 days. Data points represent mean and error bars are SEM. (**B**) Dicer$^{+/+}$aviD$^{-/-}$ or Dicer$^{-/-}$aviD$^{+/+}$ ES cells expressing GFP were transfected with a dsRNA coding for a portion of GFP or, as a negative control, encoding Renilla luciferase. GFP intensity was then measured by flow cytometry. A decrease in GFP fluorescence in dsRNA(GFP)-transfected cells compared to dsRNA(Renilla)-transfected cells represents specific silencing by RNAi (*19*). Data points represent GFP mean fluorescent intensity (MFI) in cells transfected with dsRNA(GFP) normalised on GFP MFI in cells transfected with dsRNA(Renilla). Data are mean ± SEM; $n = 3$ biological replicates. $^{**}P < 0.01$, $^{***}P < 0.001$; [two-way ANOVA in (A) and unpaired *t* test in (B)].

Figure S8

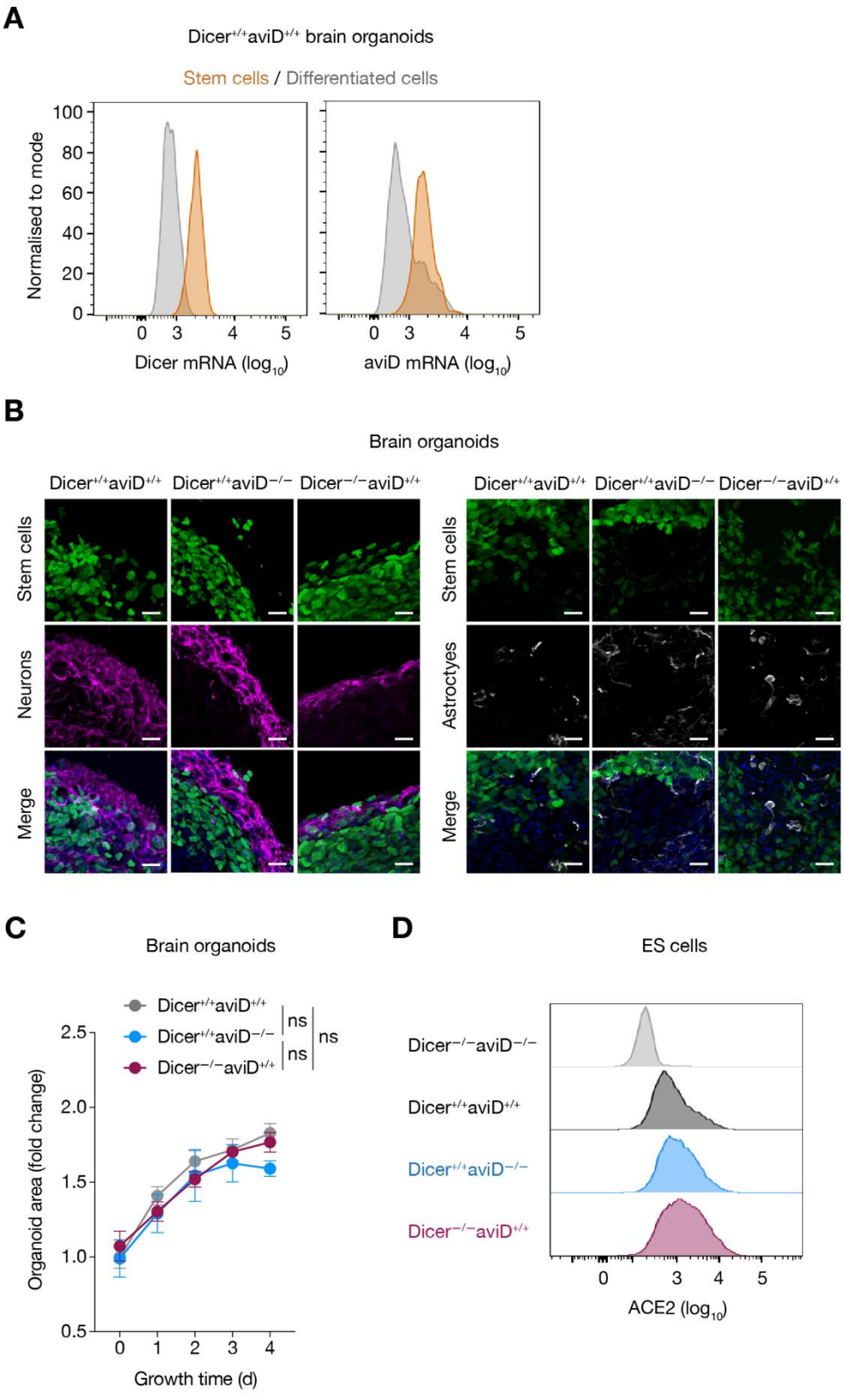
A
Dicer+/+aviD+/+ brain organoids
Stem cells / Differentiated cells
Normalised to mode
Dicer mRNA (log10)
aviD mRNA (log10)
B
Brain organoids
Dicer+/+aviD+/+
Dicer+/+aviD−/−
Dicer−/−aviD+/+
Stem cells
Neurons
Merge
Astroctyes
C
Brain organoids
ns
Organoid area (fold change)
Growth time (d)
D
ES cells
Dicer−/−aviD−/−
ACE2 (log10)

Fig. S8. Organoids from Dicer$^{+/+}$aviD$^{+/+}$, Dicer$^{+/+}$aviD$^{-/-}$ and Dicer$^{-/-}$aviD$^{+/+}$ cells show similar structure and growth kinetics in the absence of infection.

(**A**) Single cell suspensions were generated from Dicer$^{+/+}$aviD$^{+/+}$ brain organoids and Dicer or aviD mRNA was measured by PrimeFlow cytometry in stem cells marked by the expression of Sox2. Differentiated cells were identified as Sox2 negative. (**B**) Confocal imaging of Dicer$^{+/+}$aviD$^{+/+}$, Dicer$^{+/+}$aviD$^{-/-}$ and Dicer$^{-/-}$aviD$^{+/+}$ organoid sections show characteristic outer layer of neurons (left panel, TUBB3^{+}, magenta) or astrocytes (right panel, GFAP^{+}, white), as well as stem/progenitor cells (Sox2^{+}, green). Scale bar: 20 µm. (**C**) Growth of uninfected Dicer$^{+/+}$aviD$^{+/+}$, Dicer$^{+/+}$aviD$^{-/-}$or Dicer$^{-/-}$aviD$^{+/+}$ brain organoids over 4 days. Data are mean ± SEM from one of three independent experiments; *n* = 8 biological replicates. Two-way ANOVA. (**D**) Clonal ES cells Dicer$^{+/+}$aviD$^{+/+}$, Dicer$^{+/+}$aviD$^{-/-}$ and Dicer$^{-/-}$aviD$^{+/+}$ were engineered to stably express the SARS-CoV-2 receptor ACE2. Protein expression was determined by flow cytometry.

Figure S9

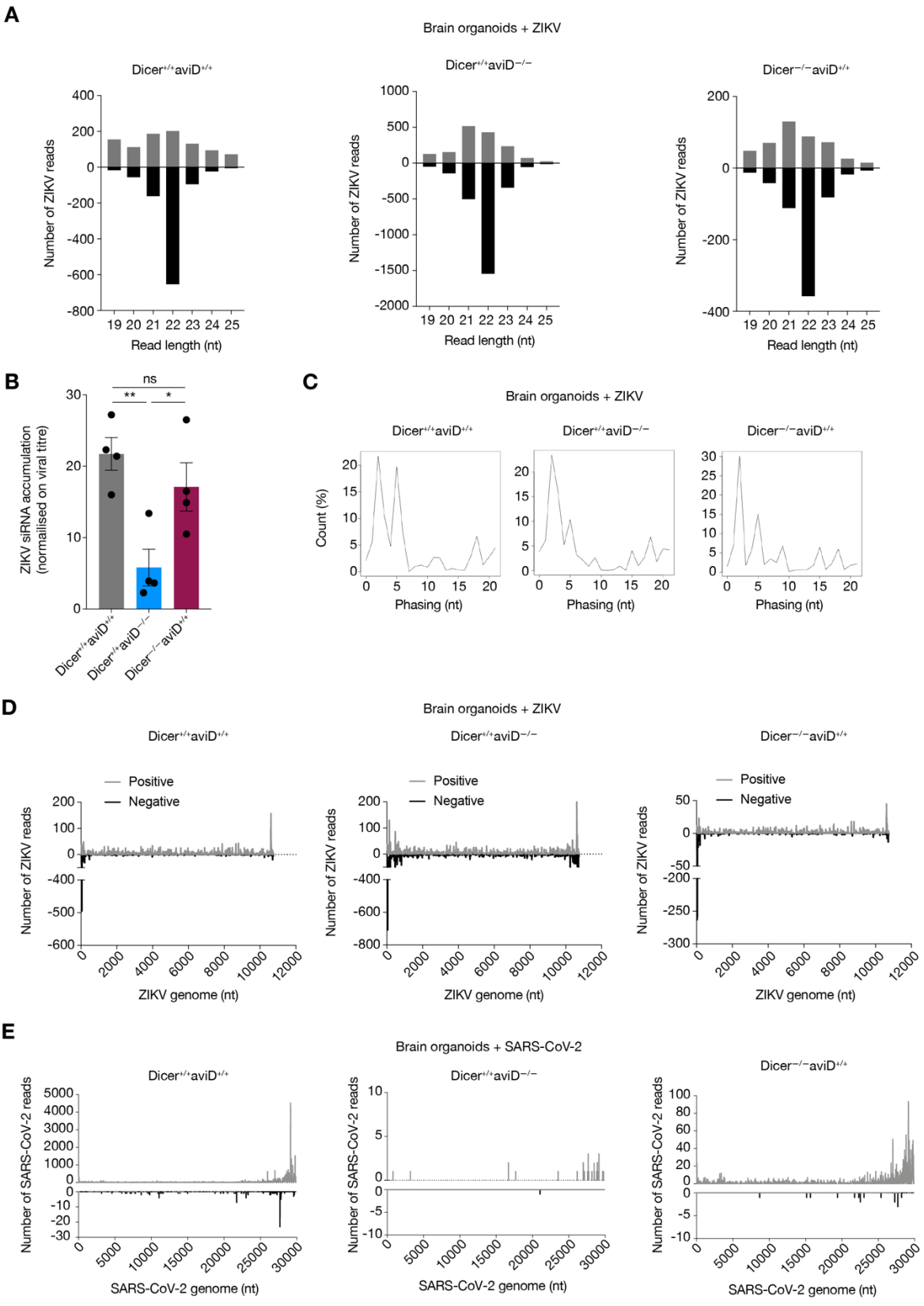
A
Brain organoids + ZIKV
Dicer+/+aviD+/+
Dicer+/+aviD−/−
Dicer−/−aviD+/+
Number of ZIKV reads
Read length (nt)
B
ns
**
*
ZIKV siRNA accumulation (normalised on viral titre)
C
Brain organoids + ZIKV
Count (%)
Phasing (nt)
D
Brain organoids + ZIKV
Positive
Negative
Number of ZIKV reads
ZIKV genome (nt)
E
Brain organoids + SARS-CoV-2
Number of SARS-CoV-2 reads
SARS-CoV-2 genome (nt)

Fig. S9. Characteristics of viral siRNAs produced in infected brain organoids.
Small RNAs from Dicer$^{+/+}$aviD$^{+/+}$, Dicer$^{-/-}$aviD$^{+/+}$ and Dicer$^{+/+}$aviD$^{-/-}$ brain organoids infected with (**A**-**D**) ZIKV for 4 days or with (**E**) SARS-CoV-2 for 2 days were analysed by next-generation sequencing. (**A**) Bar graph shows size distribution of small RNAs mapping on the ZIKV genome. (**B**) ZIKV siRNA in Dicer$^{+/+}$aviD$^{+/+}$, Dicer$^{-/-}$aviD$^{+/+}$ and Dicer$^{+/+}$aviD$^{-/-}$ brain organoids normalised by the amount of ZIKV particle produced. Data are mean ± SEM. **P* < 0.05, ***P* < 0.01, Mann-Whitney test. (**C**) Graph shows phasing analysis of 22 nucleotide-long reads mapping on ZIKV genome. (**D**) Plots shows coverage of 22 nucleotide siRNAs on ZIKV genome. (**E**) Plots shows coverage of 22 nucleotide siRNAs on SARS-CoV-2 genome.

References

1. D. Goubau, S. Deddouche, C. Reis e Sousa, Cytosolic sensing of viruses. *Immunity* **38**, 855–869 (2013). doi:10.1016/j.immuni.2013.05.007 Medline

2. J. Witteveldt, L. I. Knol, S. Macias, MicroRNA-deficient mouse embryonic stem cells acquire a functional interferon response. *eLife* **8**, e44171 (2019). doi:10.7554/eLife.44171 Medline

3. W. D'Angelo, C. Gurung, D. Acharya, B. Chen, N. Ortolano, V. Gama, F. Bai, Y.-L. Guo, The Molecular Basis for the Lack of Inflammatory Responses in Mouse Embryonic Stem Cells and Their Differentiated Cells. *J. Immunol.* **198**, 2147–2155 (2017). doi:10.4049/jimmunol.1601068 Medline

4. X.-X. Hong, G. G. Carmichael, Innate immunity in pluripotent human cells: Attenuated response to interferon-β. *J. Biol. Chem.* **288**, 16196–16205 (2013). doi:10.1074/jbc.M112.435461 Medline

5. P. V. Maillard, A. G. van der Veen, E. Z. Poirier, C. Reis e Sousa, Slicing and dicing viruses: Antiviral RNA interference in mammals. *EMBO J.* **38**, e100941 (2019). doi:10.15252/embj.2018100941 Medline

6. P. V. Maillard, C. Ciaudo, A. Marchais, Y. Li, F. Jay, S. W. Ding, O. Voinnet, Antiviral RNA interference in mammalian cells. *Science* **342**, 235–238 (2013). doi:10.1126/science.1241930 Medline

7. Y. Li, J. Lu, Y. Han, X. Fan, S.-W. Ding, RNA interference functions as an antiviral immunity mechanism in mammals. *Science* **342**, 231–234 (2013). doi:10.1126/science.1241911 Medline

8. Y. Li, M. Basavappa, J. Lu, S. Dong, D. A. Cronkite, J. T. Prior, H.-C. Reinecker, P. Hertzog, Y. Han, W.-X. Li, S. Cheloufi, F. V. Karginov, S.-W. Ding, K. L. Jeffrey, Induction and suppression of antiviral RNA interference by influenza A virus in mammalian cells. *Nat. Microbiol.* **2**, 16250 (2016). doi:10.1038/nmicrobiol.2016.250 Medline

9. Y. Qiu, Y. Xu, Y. Zhang, H. Zhou, Y.-Q. Deng, X.-F. Li, M. Miao, Q. Zhang, B. Zhong, Y. Hu, F.-C. Zhang, L. Wu, C.-F. Qin, X. Zhou, Human Virus-Derived Small RNAs Can Confer Antiviral Immunity in Mammals. *Immunity* **46**, 992–1004.e5 (2017). doi:10.1016/j.immuni.2017.05.006 Medline

10. Q. Qian, H. Zhou, T. Shu, J. Mu, Y. Fang, J. Xu, T. Li, J. Kong, Y. Qiu, X. Zhou, The Capsid Protein of Semliki Forest Virus Antagonizes RNA Interference in Mammalian Cells. *J. Virol.* **94**, e01233-19 (2019).

11. Y.-P. Xu, Y. Qiu, B. Zhang, G. Chen, Q. Chen, M. Wang, F. Mo, J. Xu, J. Wu, R.-R. Zhang, M.-L. Cheng, N.-N. Zhang, B. Lyu, W.-L. Zhu, M.-H. Wu, Q. Ye, D. Zhang, J.-H. Man, X.-F. Li, J. Cui, Z. Xu, B. Hu, X. Zhou, C.-F. Qin, Zika virus infection induces RNAi-

mediated antiviral immunity in human neural progenitors and brain organoids. *Cell Res.* **29**, 265–273 (2019). doi:10.1038/s41422-019-0152-9 Medline

12. Q. Han, G. Chen, J. Wang, D. Jee, W.-X. Li, E. C. Lai, S.-W. Ding, Mechanism and Function of Antiviral RNA Interference in Mice. *mBio* **11**, e03278-19 (2020).

13. Y. Zhang, Z. Li, Z. Ye, Y. Xu, B. Wang, C. Wang, Y. Dai, J. Lu, B. Lu, W. Zhang, Y. Li, The activation of antiviral RNA interference not only exists in neural progenitor cells but also in somatic cells in mammals. *Emerg. Microbes Infect.* **9**, 1580–1589 (2020). doi:10.1080/22221751.2020.1787798 Medline

14. Y. Qiu, Y.-P. Xu, M. Wang, M. Miao, H. Zhou, J. Xu, J. Kong, D. Zheng, R.-T. Li, R.-R. Zhang, Y. Guo, X.-F. Li, J. Cui, C.-F. Qin, X. Zhou, Flavivirus induces and antagonizes antiviral RNA interference in both mammals and mosquitoes. *Sci. Adv.* **6**, eaax7989 (2020). doi:10.1126/sciadv.aax7989 Medline

15. B. R. Cullen, S. Cherry, B. R. tenOever, Is RNA interference a physiologically relevant innate antiviral immune response in mammals? *Cell Host Microbe* **14**, 374–378 (2013). doi:10.1016/j.chom.2013.09.011 Medline

16. S. Schuster, L. E. Tholen, G. J. Overheul, F. J. M. van Kuppeveld, R. P. van Rij, Deletion of Cytoplasmic Double-Stranded RNA Sensors Does Not Uncover Viral Small Interfering RNA Production in Human Cells. *MSphere* **2**, e00333-17 (2017). doi:10.1128/mSphere.00333-17 Medline

17. K. Tsai, D. G. Courtney, E. M. Kennedy, B. R. Cullen, Influenza A virus-derived siRNAs increase in the absence of NS1 yet fail to inhibit virus replication. *RNA* **24**, 1172–1182 (2018). doi:10.1261/rna.066332.118 Medline

18. S. Schuster, G. J. Overheul, L. Bauer, F. J. M. van Kuppeveld, R. P. van Rij, No evidence for viral small RNA production and antiviral function of Argonaute 2 in human cells. *Sci. Rep.* **9**, 13752 (2019). doi:10.1038/s41598-019-50287-w Medline

19. P. V. Maillard, A. G. Van der Veen, S. Deddouche-Grass, N. C. Rogers, A. Merits, C. Reis e Sousa, Inactivation of the type I interferon pathway reveals long double-stranded RNA-mediated RNA interference in mammalian cells. *EMBO J.* **35**, 2505–2518 (2016). doi:10.15252/embj.201695086 Medline

20. A. G. van der Veen, P. V. Maillard, J. M. Schmidt, S. A. Lee, S. Deddouche-Grass, A. Borg, S. Kjær, A. P. Snijders, C. Reis e Sousa, The RIG-I-like receptor LGP2 inhibits Dicer-dependent processing of long double-stranded RNA and blocks RNA interference in mammalian cells. *EMBO J.* **37**, 97479 (2018). Medline

21. X. Wu, V. L. Dao Thi, Y. Huang, E. Billerbeck, D. Saha, H.-H. Hoffmann, Y. Wang, L. A. V. Silva, S. Sarbanes, T. Sun, L. Andrus, Y. Yu, C. Quirk, M. Li, M. R. MacDonald, W. M. Schneider, X. An, B. R. Rosenberg, C. M. Rice, Intrinsic Immunity Shapes Viral

Resistance of Stem Cells. *Cell* **172**, 423–438.e25 (2017). 10.1016/j.cell.2017.11.018 Medline

22. E. Ma, I. J. MacRae, J. F. Kirsch, J. A. Doudna, Autoinhibition of human dicer by its internal helicase domain. *J. Mol. Biol.* **380**, 237–243 (2008). doi:10.1016/j.jmb.2008.05.005 Medline

23. E. M. Kennedy, A. W. Whisnant, A. V. R. Kornepati, J. B. Marshall, H. P. Bogerd, B. R. Cullen, Production of functional small interfering RNAs by an amino-terminal deletion mutant of human Dicer. *Proc. Natl. Acad. Sci. U.S.A.* **112**, E6945–E6954 (2015). doi:10.1073/pnas.1513421112 Medline

24. M. Flemr, R. Malik, V. Franke, J. Nejepinska, R. Sedlacek, K. Vlahovicek, P. Svoboda, A retrotransposon-driven dicer isoform directs endogenous small interfering RNA production in mouse oocytes. *Cell* **155**, 807–816 (2013). doi:10.1016/j.cell.2013.10.001 Medline

25. J. E. Babiarz, J. G. Ruby, Y. Wang, D. P. Bartel, R. Blelloch, Mouse ES cells express endogenous shRNAs, siRNAs, and other Microprocessor-independent, Dicer-dependent small RNAs. *Genes Dev.* **22**, 2773–2785 (2008). doi:10.1101/gad.1705308 Medline

26. H. P. Bogerd, A. W. Whisnant, E. M. Kennedy, O. Flores, B. R. Cullen, Derivation and characterization of Dicer- and microRNA-deficient human cells. *RNA* **20**, 923–937 (2014). doi:10.1261/rna.044545.114 Medline

27. C. Gurung, M. Fendereski, K. Sapkota, J. Guo, F. Huang, Y.-L. Guo, Dicer represses the interferon response and the double-stranded RNA-activated protein kinase pathway in mouse embryonic stem cells. *J. Biol. Chem.* **296**, 100264 (2021). doi:10.1016/j.jbc.2021.100264 Medline

28. M. A. Lancaster, M. Renner, C.-A. Martin, D. Wenzel, L. S. Bicknell, M. E. Hurles, T. Homfray, J. M. Penninger, A. P. Jackson, J. A. Knoblich, Cerebral organoids model human brain development and microcephaly. *Nature* **501**, 373–379 (2013). doi:10.1038/nature12517 Medline

29. P. P. Garcez, E. C. Loiola, R. Madeiro da Costa, L. M. Higa, P. Trindade, R. Delvecchio, J. M. Nascimento, R. Brindeiro, A. Tanuri, S. K. Rehen, Zika virus impairs growth in human neurospheres and brain organoids. *Science* **352**, 816–818 (2016). doi:10.1126/science.aaf6116 Medline

30. C. Iadecola, J. Anrather, H. Kamel, Effects of COVID-19 on the Nervous System. *Cell* **183**, 16–27.e1 (2020). doi:10.1016/j.cell.2020.08.028 Medline

31. K. L. McKnight, D. A. Simpson, S.-C. Lin, T. A. Knott, J. M. Polo, D. F. Pence, D. B. Johannsen, H. W. Heidner, N. L. Davis, R. E. Johnston, Deduced consensus sequence of Sindbis virus strain AR339: Mutations contained in laboratory strains which affect cell

culture and in vivo phenotypes. *J. Virol.* **70**, 1981–1989 (1996). doi:10.1128/jvi.70.3.1981-1989.1996 Medline

32. M. C. Schwarz, M. Sourisseau, M. M. Espino, E. S. Gray, M. T. Chambers, D. Tortorella, M. J. Evans, Rescue of the 1947 Zika Virus Prototype Strain with a Cytomegalovirus Promoter-Driven cDNA Clone. *mSphere* **1**, e00246-16 (2016). 10.1128/mSphere.00246-16 Medline

33. M.-C. Saleh, M. Tassetto, R. P. van Rij, B. Goic, V. Gausson, B. Berry, C. Jacquier, C. Antoniewski, R. Andino, Antiviral immunity in Drosophila requires systemic RNA interference spread. *Nature* **458**, 346–350 (2009). doi:10.1038/nature07712 Medline

34. S. Velasco, A. J. Kedaigle, S. K. Simmons, A. Nash, M. Rocha, G. Quadrato, B. Paulsen, L. Nguyen, X. Adiconis, A. Regev, J. Z. Levin, P. Arlotta, Individual brain organoids reproducibly form cell diversity of the human cerebral cortex. *Nature* **570**, 523–527 (2019). doi:10.1038/s41586-019-1289-x Medline

35. A. D. Gracz, B. J. Puthoff, S. T. Magness, Identification, isolation, and culture of intestinal epithelial stem cells from murine intestine. *Methods Mol. Biol.* **879**, 89–107 (2012). doi:10.1007/978-1-61779-815-3_6 Medline

36. A. D. Gracz, M. K. Fuller, F. Wang, L. Li, M. Stelzner, J. C. Y. Dunn, M. G. Martin, S. T. Magness, CD24 and CD44 mark human intestinal epithelial cell populations with characteristics of active and facultative stem cells. *Stem Cells* **31**, 2024–2030 (2013). doi:10.1002/stem.1391 Medline

37. A. Cardoso, A. Gil Castro, A. C. Martins, G. M. Carriche, V. Murigneux, I. Castro, A. Cumano, P. Vieira, M. Saraiva, The Dynamics of Interleukin-10-Afforded Protection during Dextran Sulfate Sodium-Induced Colitis. *Front. Immunol.* **9**, 400 (2018). doi:10.3389/fimmu.2018.00400 Medline

38. M. A. Lancaster, N. S. Corsini, S. Wolfinger, E. H. Gustafson, A. W. Phillips, T. R. Burkard, T. Otani, F. J. Livesey, J. A. Knoblich, Guided self-organization and cortical plate formation in human brain organoids. *Nat. Biotechnol.* **35**, 659–666 (2017). doi:10.1038/nbt.3906 Medline

39. M. Martin, Cutadapt removes adapter sequences from high-throughput sequencing reads. *EMBnet J.* **17**, 10 (2011).

40. B. Langmead, C. Trapnell, M. Pop, S. L. Salzberg, Ultrafast and memory-efficient alignment of short DNA sequences to the human genome. *Genome Biol.* **10**, R25 (2009). doi:10.1186/gb-2009-10-3-r25 Medline

41. H. Li, B. Handsaker, A. Wysoker, T. Fennell, J. Ruan, N. Homer, G. Marth, G. Abecasis, R. Durbin, 1000 Genome Project Data Processing Subgroup, The Sequence Alignment/Map format and SAMtools. *Bioinformatics* **25**, 2078–2079 (2009). doi:10.1093/bioinformatics/btp352 Medline

42. A. R. Quinlan, I. M. Hall, BEDTools: A flexible suite of utilities for comparing genomic features. *Bioinformatics* **26**, 841–842 (2010). doi:10.1093/bioinformatics/btq033 Medline

43. J. Lemon, Plotrix: A Package in the Red Light District of R. *R News* **6**, 8–12 (2006).